*31st EPS Conference on Plasma Phys. London, 28 June - 2 July 2004 ECA Vol.**28G**, P-1.034 (2004)*

Control of ion and cation fluxes in low-temperature deposition of ordered carbon nanostructures

I. B. Denysenko[1,2], S. Xu[3], K. Ostrikov[3,4], M. Y. Yu[1]

[1] Theoretical Physics I, Ruhr University, D-44780 Bochum, Germany; [2] Kharkiv National University, Kharkiv, Ukraine; [3]Plasma Sources and Applications Center, NIE, Nanyang Technological University, 637616 Singapore; [4]School of Physics, The University of Sydney, Sydney, NSW 2006, Australia.

Properties of inductively coupled (IC) $Ar/CH_4/H_2$ 0.46 MHz plasmas have been investigated both experimentally and numerically. The plasma is produced in a cylindrical stainless steel reactor chamber with the inner diameter $2R$ = 32 cm and length 23 cm. The top plate of the chamber is a fused silica disk, 35 cm in diameter and 1.2 cm thick. The inductive coils are placed on the disk. A top surface of the stainless steel substrate holder of the diameter 17.5 cm is located 11 cm below the bottom surface of the quartz window.

The plasma study is carried out at conditions typical for growth of self-assembled vertically aligned carbon nanostructures (CNs) [1]. A typical scanning electron micrograph of the PECVD-grown ordered vertically aligned carbon nanotip structure is shown in Fig. 1 (a), and the typical parameters corresponding to CNs growth are given in the caption to the figure. Variations of neutral densities with the input parameters are measured by a Microvision Plus LP101009 Quadrupole Mass Spectrometer (QMS) equipped with a Faraday cup detector. A typical distribution of the radical and non-radical neutral species in the PECVD of the self-assembled ordered carbon nanotip arrays is shown in Fig. 1 (b).

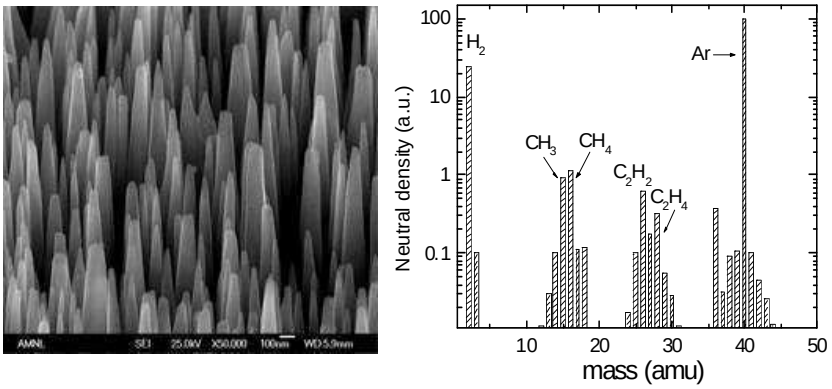

(a) (b)

Fig.1. (a) High-resolution scanning electron micrograph of carbon nanotip array deposited in the IC plasma of $Ar/CH_4/H_2$ mixture at absorbed power in the discharge P_{in} = 2 kW, argon J_{Ar} = 35 sccm, hydrogen J_{H2} = 12.4 sccm, and methane J_{CH4}= 7.5 sccm input flow rates, respectively, the DC voltage applied to the substrate holder V_s=-300 V, and the substrate temperature T_s=300 C; (b) Mass spectrum of the neutrals measured by QMS in the $Ar/CH_4/H_2$ plasma for the same conditions as in Fig.1 (a).

A spatially averaged (global) model has been developed to calculate the charged and neutral particle densities in the IC plasma of $Ar/CH_4/H_2$ gas mixtures. In the model it is assumed that the main species in the discharge are: Ar, H_2, CH_4, C_2H_2, C_2H_4, C_2H_6, C_3H_8 (7 non-radical neutrals), H,CH,CH_2,CH_3,C_2H_5 (5 radical neutrals), H^+, H_2^+, H_3^+,CH_3^+, CH_4^+,CH_5^+, $C_2H_2^+$, $C_2H_4^+$,$C_2H_5^+$,Ar^+ (10 cations) and electrons. The electron energy distribution function is assumed Druyvesteyn-like. The overall charge neutrality

$$\sum_i n_i = n_e \qquad (1)$$

is implied, where n_e and n_i are the number densities of the electrons and cation species i, respectively. The balance equation for neutrals is

$$0 = I_n - O_n - \sum_i k_i n_e n_n + \sum_{jkm} k_j n_k n_m - \sum_{ls} k_l n_s n_n + 0.5 K^H_{wall} n_H - K^n_{wall} n_n \qquad (2)$$

where I_n and O_n are the inflow and the outflow per unit time of the n molecules in the discharge. The third term in the RHS of (2) accounts for the loss in electron impact reactions, whereas the fourth and fifth terms account for the gain and loss from the neutral/ion-neutral reactions, respectively. The 6th term in (2) does not equal to zero only in the H_2 balance equation and reflects the fact that atomic hydrogen usually converts into a molecular state after reaction with the chamber wall. Here, $K^n_{wall} n_n$ is the number of neutral species n lost on the discharge wall per unit time per unit volume. It is nonzero only for radical neutrals. The balance equation for the cation species and the electron power balance equation can be found elsewhere [2].

Using the set (1), (2), and the cation and power balance equations the densities of neutral and charged species for different input powers and input flow rates were calculated. Figs. 2(a) and (b) show the calculated densities of neutrals and ions. The QMS measured neutral densities are depicted in Fig. 2 (c). It is seen that the ion, neutral and radical densities in the discharge can be efficiently controlled by the input power.

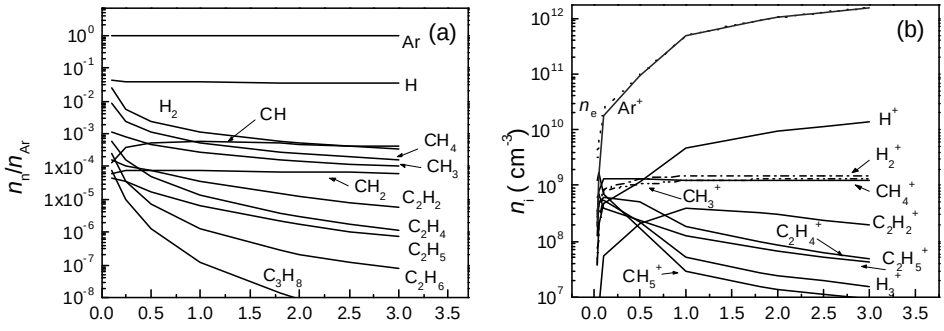

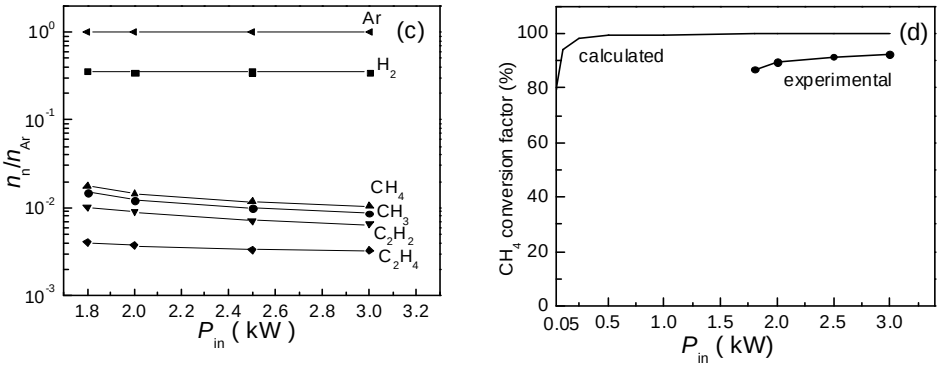

Fig.2. Normalized computed (a) and QMS measured (c) densities of neutrals, computed ion densities (b), and computed and QMS measured CH_4 conversion factor (d) as functions of the power input P_{in} for the same gas feedstock as in Fig.1.

The electron, Ar^+ and H^+ densities increase with power. Meanwhile, the densities of most of hydrocarbon neutrals drop with P_{in} due to the enhancement of their collisions with the plasma electrons and ions. Ar is a dominant neutral species in the discharge. The density of hydrogen atoms is approximately 25 times smaller than the argon density and slightly decreases with power. As can be seen in Fig. 2(a), the density of molecular hydrogen at low input powers is comparable to that of atomic hydrogen, and also diminishes with P_{in}. The latter decrease can be attributed to the enhanced dissociation of hydrogen molecules at higher input powers accompanied by the rise in the electron number density [Fig.2(b)]. Under the CN growth conditions, the hydrogen conversion factor (degree of dissociation) approaches 99 %. A comparison between the experimental and calculated values of CH_4 conversion factor at variable Rf power in Fig. 2(d) shows a consistent tendency to rise with power. Apparently, the high CH_4 conversion factors in the power range for the CN growth (1.8-3 kW) are due to the high densities of atomic hydrogen at elevated electron densities in hydrogen-containing plasmas, which promotes intensive chemical reactions between H and CH_4. An increase of the input argon flow rate is accompanied by the rise of the densities of electrons, Ar^+, and hydrocarbon neutrals and cations. On the contrary, the effective electron temperature (T_{eff} = 4.27, 3.87, 3.6, and 3.45 eV for P_{in}= 2 kW, J_{CH4} = 6.0 sccm, J_{H2} = 12.4 sccm, and J_{Ar} = 10, 20, 35, and 50 sccm, respectively) and the densities of the atomic and molecular hydrogen neutrals and H^+ cations decline with J_{Ar}. Higher inflow of the carbon source gas CH_4 naturally enhances the generation of C_xH_y cations and radical neutrals (here x=1-2 and y= 1-6, and 8). Thus, various inelastic collisional processes intensify, which results in somewhat lower electron number densities. Furthermore, the electron-impact reactions involving a larger number of C_xH_y neutrals yield larger amounts of atomic hydrogen, the latter contributes to higher densities of H_2 as a result of C_xH_y + H reactions.

The computed ion and radical neutral densities have been used to analyze the fluxes of different species onto the catalyzed substrate in the CN PECVD process. We compare the numbers of the radical neutrals deposited per unit time per unit surface $\Psi_n^j = 0.25 n_j \gamma_j \upsilon_{thj}$ (where γ_j and υ_{thj} are the sticking coefficient and thermal velocity for corresponding radical neutral) with those of the plasma ions $\Psi_i = h_L n_i \upsilon_{Bi}$. Here h_L is the ratio of the density of the cation *i* on the outer surfaces of the cylindrical plasma column in the axial ($z=0,L$) direction to the bulk averaged density n_i, respectively. u_{Bi} is the velocity of ion species *i* at the plasma - sheath edge. Indexes *j* and *i* denote radical and ion species, respectively. The total flux density of the hydrocarbon radical neutrals Ψ_n strongly depends on the input power. At P_{in}=50 W and the other parameters as in Fig.1, $\Psi_n \approx 1.63\times10^{14}$ $s^{-1}cm^{-2}$ and further grows to 2.55×10^{14} $s^{-1}cm^{-2}$ at 0.5 kW. In the subsequent power range (0.5-3.0 kW) the flux density declines with power. For instance, Ψ_n = 2.42, 1.98, 1.62 $s^{-1}cm^{-2}$ at P_{in} = 1, 2, and 3 kW, respectively. The total flux density of hydrocarbon ions onto the processing surface Ψ_i is slightly higher than Ψ_n and drops with P_{in} in the entire power range of interest here. Specifically, Ψ_i = 3.66, 3.14, 3.02, 2.85, 2.75 $\times10^{14}$ $s^{-1}cm^{-2}$ at P_{in} = 0.05, 0.5, 1, 2, and 3 kW, respectively. The numerics reveal that total hydrocarbon neutral flux Ψ_n is approximately 1.5 times smaller than the ion one Ψ_i in a typical carbon nanotip growth process with P_{in} =1.8-3.0 kW, J_{CH4}=7.5 sccm, J_{H2}=12.4 sccm, and J_{Ar}=35 sccm. Varying the inflow rates of methane and argon, one can control the ratio Ψ_i/Ψ_n. The total fluxes of the ion and neutral hydrocarbon species naturally grow with J_{CH4}. At low methane inlets (J_{CH4} =4.5 sccm) $\Psi_i \approx \Psi_n$, whereas at higher J_{CH4} the deposited flux of hydrocarbon cations can be ~ 20% higher than the neutral flux. An increase of the argon input flow rate results in a pronounced growth of Ψ_n and diminishing of Ψ_i.

In conclusion, we note that the ion, neutral and radical densities in the discharge can be efficiently controlled by the input power and methane/argon input flow rates. The ion fluxes onto the substrate in the CN growth process can exceed those of the neutral species and thus play a crucial role in the growth of nanonostructured carbon-based films.

Acknowledgments. The work of I.B.D. was supported by the A. von Humboldt Foundation. This work was partially supported by the Australian Research Council, The University of Sydney, A*STAR (Singapore), AcRF (NTU, Singapore), Lee Kuan Yew Foundation, and the NATO.

[1] Z. L. Tsakadze, K. Ostrikov, and S. Xu, Surf. Coat. Technol. *accepted for publication* (2004).
[2] C. Lee and M. A. Lieberman, J.Vac. Sci. Technol. A , **13**, 368 (1995).